Supplementary Information: Room temperature coherent control of implanted defect spins in Silicon carbide

Fei-Fei Yan,[1,3,*] Ai-Lun Yi,[2,4,*] Jun-Feng Wang,[1,3] Qiang Li,[1,3] Pei Yu,[1,5,6] Jia-Xiang Zhang,[2,4] Adam Gali,[7,8] Ya Wang,[1,5,6] Jin-Shi Xu,[1,3,†] Xin Ou,[2,4,‡] Chuan-Feng Li,[1,3,§] and Guang-Can Guo[1,3]

[1] *Synergetic Innovation Center of Quantum Information and Quantum Physics, University of Science and Technology of China, Hefei 230026, People's Republic of China*

[2] *State Key Laboratory of Functional Materials for Informatics, Shanghai Institute of Microsystem and Information Technology, Chinese Academy of Sciences, Shanghai, 200050, People's Republic of China*

[3] *CAS Key Laboratory of Quantum Information, University of Science and Technology of China, Hefei 230026, People's Republic of China*

[4] *Center of Materials Science and Optoelectronics Engineering, University of Chinese Academy of Sciences, Beijing, 100049, People's Republic of China*

[5] *CAS Key Laboratory of Microscale Magnetic Resonance and Department of Modern Physics, University of Science and Technology of China, Hefei 230026, China.*

[6] *Hefei National Laboratory for Physical Sciences at the Microscale, University of Science and Technology of China, Hefei 230026, China.*

[7] *Department of Atomic Physics, Budapest University of Technology and Economics, Budafoki út. 8, H-1111, Hungary*

[8] *Wigner Research Center for Physics, PO. Box 49, H-1525, Hungary*

(Dated: March 26, 2020)

* These authors contributed equally to this work.

† jsxu@ustc.edu.cn

‡ ouxin@mail.sim.ac.cn

§ cfli@ustc.edu.cn

I. ANALYSIS OF THREE-LEVEL SYSTEM AND FOUR-LEVEL SYSTEM

For a four-level system, the ground-state spin Hamiltonian can be expressed as follows [1]

$$H = D\left[S_z^2 - \frac{S(S+1)}{3}\right] + E(S_x^2 - S_y^2) + g\mu_B \vec{\mathbf{B}}_0 \cdot \vec{\mathbf{S}}, \tag{1}$$

where the Landé g-factor of the electron spin is 2.0028, μ_B is the Bohr magneton, and $\vec{\mathbf{B}}_0$ denotes the applied external magnetic field; D and E are the zero-field-splitting (ZFS) parameters. For the four-level system with $S = 3/2$ and $m_s = +3/2$, $+1/2$, $-1/2$ and $-3/2$, the Hamiltonian matrix at zero magnetic field can be written as

$$\begin{bmatrix} D & 0 & \sqrt{3}E & 0 \\ 0 & -D & 0 & \sqrt{3}E \\ \sqrt{3}E & 0 & -D & 0 \\ 0 & \sqrt{3}E & 0 & D \end{bmatrix}.$$

The eigenvalues and corresponding eigenstates ($|S, m_s\rangle$) of this spin Hamiltonian matrix are given by

$$\sqrt{3E^2 + D^2} \text{ for } \left|\frac{3}{2}, \frac{3}{2}\right\rangle,$$

$$-\sqrt{3E^2 + D^2} \text{ for } \left|\frac{3}{2}, \frac{1}{2}\right\rangle,$$

$$-\sqrt{3E^2 + D^2} \text{ for } \left|\frac{3}{2}, -\frac{1}{2}\right\rangle,$$

$$\sqrt{3E^2 + D^2} \text{ for } \left|\frac{3}{2}, -\frac{3}{2}\right\rangle.$$

It can be observed that the states of $m_s = \pm 1/2$ and $m_s = \pm 3/2$ are degenerate at zero magnetic field. Thus, only one resonant transition ($2\sqrt{3E^2 + D^2}$) can be observed between $m_s = \pm 1/2$ and $m_s = \pm 3/2$, even when E is not zero.

Meanwhile, for a three-level system ($S = 1$), the ground-state spin Hamiltonian can be expressed as follows [2]:

$$H = DS_z^2 - E(S_x^2 - S_y^2) + g\mu_B \vec{\mathbf{B}_0} \cdot \vec{\mathbf{S}}. \tag{2}$$

The corresponding Hamiltonian matrix at zero magnetic field can be written as

$$\begin{bmatrix} D & 0 & E \\ 0 & 0 & 0 \\ E & 0 & D \end{bmatrix}.$$

The eigenvalues and corresponding eigenstates ($|S, m_S\rangle$) of this spin Hamiltonian matrix are given by

$$D + E \text{ for } |1, 1\rangle,$$

$$0 \text{ for } |1, 0\rangle,$$

$$D - E \text{ for } |1, -1\rangle.$$

The states of $m_s = \pm 1$ are not degenerate when E is not equal to zero, and two resonant transitions ($|D + E|$ and $|D - E|$) are observed, which is the case for the observed PL8 defects. Thus, the ground state of PL8 defect spins can be classified as a three-level system.

II. MORE EXPERIMENTAL RESULTS FOR THE IMPLANTED HYDROGEN ION SAMPLE

The photoluminescence (PL) spectra of PL8 defects in samples implanted with 170-keV H^+ with different fluences are shown in Fig. 1(a). With the increase of the implanted fluence, the full width at half maximum (FWHM) of the zero-phonon line (ZPL) broadened. To investigate other photoluminescence peaks, we detected the photoluminescence spectra of samples with different anneal times, as shown in Fig. 1(b). The ZPL belonging to the defect investigated in this work was denoted as PL8, while the other peaks were designated from U1 to U7. For different samples, we normalize the intensity of PL8. We found that the intensities of U1 to U7 did not proportionally change; in fact, U4 and U7 even disappeared in some cases. Therefore, we conclude that peaks U1 to U7 were not related to the defect investigated in this work. Furthermore, we measured the lifetime of PL8 defects in a sample implanted with 170-keV hydrogen ions (H^+) with a fluence of 1×10^{16} cm^{-2} and annealed at 1,300°C. During the detection, only ZPL at 1,007 nm was collected via a band-pass filter from 1,000 to 1,024 nm. As shown in Fig. 1(c), the optical decay time T_{opt}

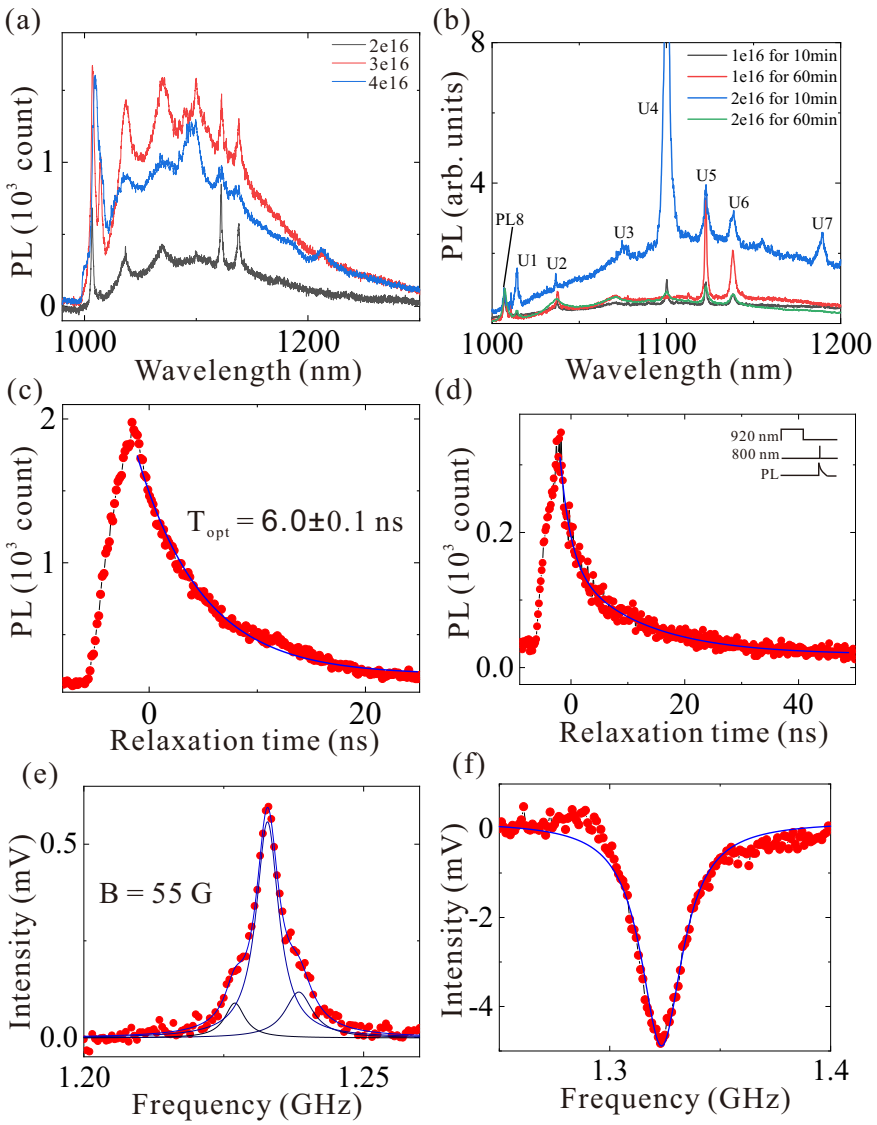

FIG. 1. **Optical lifetime and spin property of PL8 defects.** (a) Photoluminescence spectra of samples implanted by different fluences at 20 K. The width of ZPL lines become broaden with the increase of fluence. (b) The photoluminesence spectra of different samples for comparing different peaks. (c) The lifetime measurement at 10 K. Only fluorescence from the ZPL is collected. The single exponential decay fitting reveals that $T_{\rm opt} = 6.0 \pm 0.1$ ns. (d) Measurement of the spin polarization at 10 K. We first polarized state to $|0\rangle$ with a 4 μs-long 920-nm laser pulse. After waiting for 4 μs, we measure the fluorescence lifetime. Only the fluorescence from the ZPL is collected. From the bi-exponential decay fitting, we obtain the spin polarization to be 97.5%. (e) Pulse ODMR for the PL8 defects at room temperature with 55 G magnetic field. Nuclear spins coupling at 1227.0 $\pm$ 0.2 MHz, 1238.4 $\pm$ 0.3 MHz are deduced from the Lorenz fittings. (f) ODMR spectrum of the sample implanted by 170-keV hydrogen ions with a fluence of 1×10^{15} cm^{-2} and annealed at 900 °C for 30 min.

= 6.0 ns was deduced from the theoretical fitting, which was shorter than that of the divacancies of 14 ns (see Table I). We also measured the spin polarization. A 920-nm laser pulse with 4-μs duration was used to initialize PL8 defects. After waiting for 4 μs, the lifetime was measured [3, 4]. From the bi-exponential decay fitting (Fig. 1(d)), the spin polarization was deduced to be 97.5%. We implemented the pulse optically detected magnetic resonance (ODMR) measurement at 55-G magnetic field. The spectrum is shown in Fig. 1(e). The resonant frequency was fitted as 1,232.8 MHz with an FWHM of 4.9 MHz. Two nuclear couplings at 1,227 and 1,238 MHz were observed. Fig. 1(f) shows the ODMR spectrum for the lower annealing temperature at 900°C for 30 min. Only ODMR signal of the divacancy center of PL1 was observed at 1,323.5 MHz.

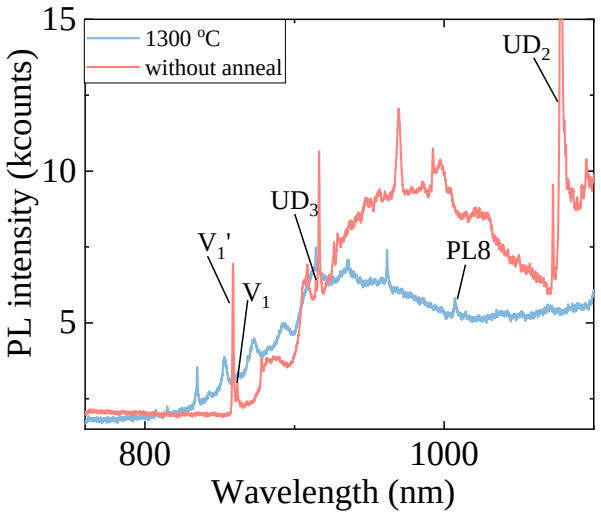

FIG. 2. The PL spectra of samples excited with 532-nm laser. The blue line and red line represent the PL spectra of samples annealed at 1300 °C and without annealing at 10 K.

We also measured the PL spectra of samples using 532-nm laser pumping at 10 K, as shown in Fig. 2. One of the samples was implanted with 170-keV H^+ with a dose of 1×10^{15} cm^{-2} and without annealing (red line), while the other sample was implanted with 170-keV H^+ with a dose of 2×10^{16} cm^{-2} and annealed at 1300°C (blue line). Compared with the work of Rühl et al. [5], we only observed V lines and UD lines; TS lines were not observed, possibly because they were sample-related. Moreover, after 1,300°C annealing, ZPL of PL8 spectrum was observed, but some peaks disappeared.

III. SAMPLES IMPLANTED WITH OTHER IONS

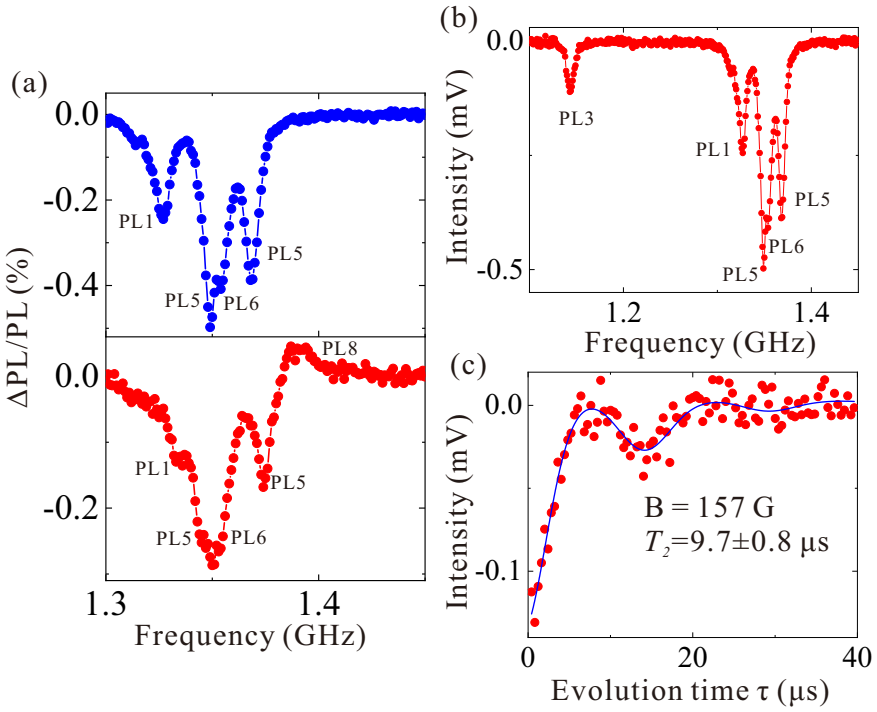

FIG. 3. **Spin properties of defects implanted by He^+ and C^+ at room temperature.** (a) ODMR spectra of samples implanted by 170-keV He^+ with the fluence of 5×10^{15} cm^{-2} (blue dots) and 2×10^{16} cm^{-2} (red dots) . Divacancy defect signals (1,324.7 MHz for PL1, 1,344.4 MHz for PL5, 1,351.9 MHz for PL6 and 1,374.5 MHz for PL5) are observed for both cases. But PL8 defect signal is only observed with lower implanted fluence. (b) ODMR spectrum of the sample implanted by 40 keV C^+ with the fluence of 1×10^{14} cm^{-2}. Only the divacancy defect signals (1,326.3 MHz for PL1, 1,143.6 MHz for PL3, 1,349.3 MHz for PL5, 1,356.9 MHz for PL6 and 1,368.4 MHz for PL5) are observed. There are not PL8 defects. (c) The Hahn echo spin coherence time of PL6 in (b) measured at 157 G magnetic field. $T_2 = 9.7 \pm 0.8$ μs is deduced from the fit.

For comparison, we measured the spin properties of the defects in samples implanted with He^+ and C^+, which were annealed at 1,300°C for 2 h. The samples were excited using 920-nm laser, and the fluorescence was collected using 1,000-nm longpass filter. The red and blue dots in Fig. 3(a) represent the experimental results of ODMR signals of samples implanted with 170-keV He^+ with a fluence of 5×10^{15} cm^{-2} and 2×10^{16} cm^{-2}, respectively. Divacancy defect signals (1,324.7 MHz for PL1, 1,344.4 MHz for PL5, 1,351.9 MHz for PL6, and 1,374.5 MHz for PL5, the resonance frequency will be different because of the internal stress, but the ZFS parameter D remains constant.) were observed in both cases. However, the PL8 defect signal was observed only

with a lower implanted fluence. The ODMR spectrum of the sample implanted with 40-keV C^+ with a fluence of 1×10^{14} cm^{-2} is shown in Fig. 3(b). There were no signals from PL8 defects. The observed ZFS parameters D and E of the divacancy defects were changed owing to the stress change after annealing at 1,300°C. Fig. 3(c) shows the Hahn echo spin coherent time of PL6 obtained in Fig. 3(b) with 157-G magnetic field. T_2 was shown to be 9.7 ± 0.8 μs, i.e., as long as that of the PL8 defect spins.

PL name	EPR name	Identification	Orientation	ZPL (nm)	D (MHz) LT	D (MHz) RT	E (MHz)	Room temp?	optical lifetime (ns)	annealed temp (°C)
PL1	P6b	(hh) divacancy	$c-$axis	1132	1336	1323.5	<1	implanted	15	750 °C in Ar gas for 30 min
PL2	P6′b	(kk) divacancy	$c-$axis	1131	1305	-	<1	no	15	750 °C in Ar gas for 30 min
PL3	P7b	basal divacancy	basal	1108	1222	-	82	no	12	750 °C in Ar gas for 30 min
PL4	P7′b	basal divacancy	basal	1078	1334	-	18.7	no	14	750 °C in Ar gas for 30 min
PL5	-	unknown	basal	1043	1373	1358	16.5	yes	13	-
PL6	-	unknown	$c-$axis	1038	1365	1352	<1	yes	14	-
PL7*	-	unknown	basal	-	-	-	-	yes	-	-
PL8	-	unknown	$c-$axis	1007	1398.7	1387.8	4	yes	6.0	proton implanted and 1300 annealed
NV	-	-	-	637	2878	2871	7.5	yes	15.7	-

* Only one ODMR dip is detected

TABLE I. **ZPL, ZFS, and optical lifetime of vacancy in 4H-SiC.** LT and RT refer to low-temperature and room-temperature. The data for PL1 to PL7 are from Ref. [6, 7]. ZPL and ZFL data for NV center are from Ref. [8, 9]; the lifetime for the NV center is from Ref. [10].

[1] Widmann, M. *et al.* Coherent control of single spins in silicon carbide at room temperature. *Nature Mat.* **14**, 164 (2015).

[2] Christle, D. J. *et al.* Isolated electron spins in silicon carbide with millisecond coherence times. *Nature Mat.* **14**, 160 (2015).

[3] Klimov, P. V. *et al.* Quantum entanglement at ambient conditions in a macroscopic solid-state spin ensemble. *Sci. Adv.* **1,** e1501015 (2015).

[4] Robledo, L. *et al.* Spin dynamics in the optical cycle of single nitrogen-vacancy centres in diamond. *New Journal of Phys.* **13,** 025013 (2011).

[5] Rühl, M. *et al.* Controlled generation of intrinsic near-infrared color centers in 4H-SiC via proton irradiation and annealing. *Appl. Phys. Lett.* **113,** 122102 (2018).

[6] Falk, A. L. *et al.* Polytype control of spin qubits in silicon carbide. *Nature Commun.* **4,** 1819 (2013).

[7] Falk, A. L. *et al.* Electrically and mechanically tunable electron spins in silicon carbide color centers. *Phy. Rev. Lett.* **112,** 187601 (2014).

[8] Gruber, A. *et al.* Scanning confocal optical microscopy and magnetic resonance on single defect centers. *Science* **276,** 2012 (1997).

[9] Chen, X.D. *et al.* Temperature dependent energy level shifts of nitrogen-vacancy centers in diamond. *Appl. Phys. Lett.* **99,** 161903 (2011).

[10] Li, D. F. *et al.* Thickness dependent surface plasmon of silver film detected by nitrogen vacancy centers in diamond. *Opt. Lett.* **22,** 5587 (2018).